Particle manipulation by a non-resonant acoustic levitator

Marco A. B. Andrade,[1,a)] Nicolás Pérez,[2] and Julio C. Adamowski[3]

[1]Institute of Physics, University of São Paulo, CP 66318, 05314-970 São Paulo, Brazil
[2]Centro Universitario de Paysandú, Universidad de la República, Ruta 3 km 363, 60000 Paysandú, Uruguay
[3]Department of Mechatronics and Mechanical Systems Engineering, Escola Politécnica,
University of São Paulo, Av. Mello Moraes, 2231, 05508-030 São Paulo, Brazil

We present the analysis of a non-resonant acoustic levitator, formed by an ultrasonic transducer and a concave reflector. In contrast to traditional levitators, the geometry presented herein does not require the separation distance between the transducer and the reflector to be a multiple of half wavelength. The levitator behavior is numerically predicted by applying a numerical model to calculate the acoustic pressure distribution and the Gor'kov theory to obtain the potential of the acoustic radiation force that acts on a levitated particle. We also demonstrate that levitating particles can be manipulated by controlling the reflector position while maintaining the transducer in a fixed position. © 2015 AIP Publishing LLC. [http://dx.doi.org/10.1063/1.4905130]

Acoustic levitation[1] of small particles and liquid droplets has a wide range of applications in biology,[2] analytical chemistry,[3,4] pharmacy,[5,6] and in other fields.[7–9] Until recently, acoustic levitation was used almost exclusively to trap particles in the air. But in the last few years, acoustic levitation devices have been developed to suspend and to manipulate particles,[10–14] which can significantly increase the applicability of acoustic levitation.

The most common type of acoustic levitator is called single-axis,[15] and it consists of a circular ultrasonic transducer and a reflector. In this levitator, the distance between the transducer and the reflector should be carefully adjusted such that a standing wave is formed between the transducer and the reflector. By assuming a plane wave, the separation distance should be adjusted to a multiple of half wavelength, and once a standing wave is established, the wave produces an acoustic radiation force that pushes a small particle to a pressure node of the standing wave field. When the distance between the transducer and the reflector is adjusted outside the resonance, the acoustic radiation force that acts on the levitated particle is not strong enough to maintain the particle levitating.

A non-resonant acoustic levitator was proposed by Rey.[16,17] In a typical single-axis acoustic levitator, the standing wave is formed by the multiple wave reflections that occur between the transducer and the reflector. In the non-resonant levitator, the standing wave is mainly formed by the superposition of two waves: the emitted wave by the transducer and the first reflected wave. The interference between these two waves creates a pressure node near the reflector surface, and a small particle can be levitated near the reflector. The small size of the reflector minimizes the multiple reflections, and the acoustic radiation force that acts on the levitated particles is almost independent of the distance between the transducer and the reflector.

A standing wave field can also be generated by the superposition of counter-propagating waves emitted by two opposed transducers.[18–20] In this approach, the nodal positions can be controlled by changing the phase difference between the two transducers, which allows manipulating small particles electronically. Devices based on counter-propagating waves can be used to manipulate small particles in liquids[18,20] and in the air.[14,19]

In this letter, we present a non-resonant acoustic levitator based on the levitation concept proposed by Rey.[16] Compared to prior devices, our acoustic levitator has the main feature of being robust to perturbations, and the separation distance between the transducer and the reflector can be adjusted continuously, without losing the levitation capability. In our setup, a concave reflector is used to increase the axial and lateral forces that act on the levitated particles. This configuration allows the direct manipulation of small particles by changing the reflector position. The levitation behavior is investigated by using a 3D numerical model to determine the potential of the acoustic radiation force that acts on the levitated particles.

The acoustic levitator is illustrated in Fig. 1 and consists of two main parts: a piezoelectric transducer with a flat vibrating surface of 10-mm diameter and a concave reflector
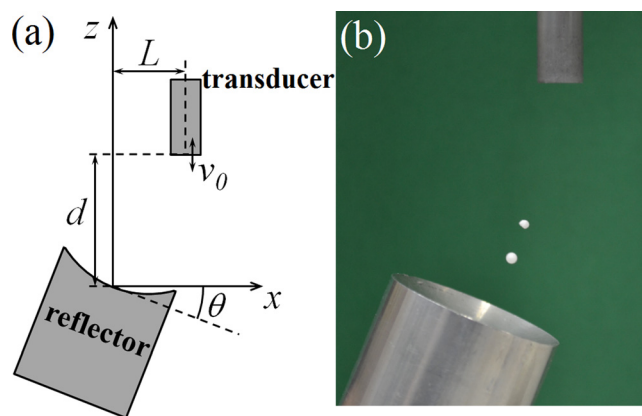

FIG. 1. (a) Schematic diagram of the acoustic levitator. (b) Acoustic levitation of two expanded polystyrene particles. The multimedia view is a demonstration video. (Multimedia view) [URL: http://dx.doi.org/10.1063/1.4905130.1]

a)Author to whom correspondence should be addressed. Electronic mail: marcobrizzotti@gmail.com

of 40-mm diameter with a curvature radius of 33 mm. The transducer surface vibrates harmonically with a velocity amplitude v_0 at a frequency of approximately 23.7 kHz. The distance between the transducer and the reflector is d, and the reflector can be displaced off-axis by a distance L and tilted by an angle θ, as illustrated in Fig. 1(a). By maintaining the transducer in a fixed position, the reflector can be moved up and down for a distance of more than 50 mm, without significantly affecting the levitation performance. A demonstration video of this levitator is available online (Fig. 1).

To understand the levitator behavior, the Gor'kov theory[21] is applied to calculate the potential of the acoustic radiation force that acts on a small sphere. This theory requires the knowledge of the acoustic pressure distribution in the air gap between the transducer and the reflector, which is obtained numerically by a matrix method[22,23] based on the Rayleigh integral. Seah et al.[14] applied a similar model to simulate an ultrasonic manipulation device. The numerical simulations performed by Seah et al.[14] assume that each ultrasonic transducer emits a wave into the free space. In contrast, our model is able to simulate the high-order reflections that occur between the transducer and the reflector. According to the Gor'kov theory, the acoustic radiation force produced by a standing wave that acts on a sphere with a size much smaller than the wavelength can be calculated from the Gor'kov potential U, given by[21]

$$U = 2\pi R^3 \left[\frac{\langle p^2 \rangle}{3\rho c^2} - \frac{\rho \langle u^2 \rangle}{2} \right], \tag{1}$$

where R is the radius of the sphere, ρ is the air density, c is the sound velocity of the air, and $\langle p^2 \rangle$ and $\langle u^2 \rangle$ are the mean square amplitudes of the sound pressure and velocity, respectively. The Gor'kov theory is useful to predict the levitation positions of small particles in a standing wave field. If gravity is neglected, small particles are trapped in the positions of minimum Gor'kov potential. In this letter, we apply the dimensionless form of U, given by[15]

$$\tilde{U} = \frac{U}{2\pi R^3 \rho v_0^2}. \tag{2}$$

The advantage of using the dimensionless potential $\tilde{U}$ is that it is independent of the sphere radius R and the transducer velocity amplitude v_0.

Before determining the Gor'kov potential, the matrix method[22,23] was applied to simulate the wave propagation inside the levitator. This method allows performing 3D simulations of the pressure field in a few seconds. In this method, the pressure distribution is determined by summing the multiple wave reflections that occur between the transducer and the reflector. The dimensionless form of the pressure $\tilde{p} = p/\rho c v_0$ was obtained by considering an air density of 1.2 kg/m^3 and a sound velocity of 340 m/s. The wave emitted by the transducer is illustrated in Fig. 2(a). Figure 2(b) shows the pressure after the first reflection and Fig. 2(c) shows the wave after the second reflection. Figure 2(d) shows the modulus of the dimensionless pressure, which corresponds to the sum of the three previous waves. As observed in Fig. 2, the main contributions to the total pressure distribution are the emitted and the first reflected waves. The second reflected wave has a small influence on the total pressure distribution. Due to the small radius of the transducer surface, the first reflected wave is almost completely spread into the surrounding medium and only a small portion is reflected back by the transducer surface. In the present setup, numerical simulations show that for $d > 50$ mm, less than 3% of the total energy is reflected back by the transducer surface. In this condition, we can consider that the standing wave is formed by the superposition of the emitted wave and the first reflected wave. For values of d below 30 mm, higher order reflections become significant and the levitator starts to present a resonant behavior. Another consequence of the small
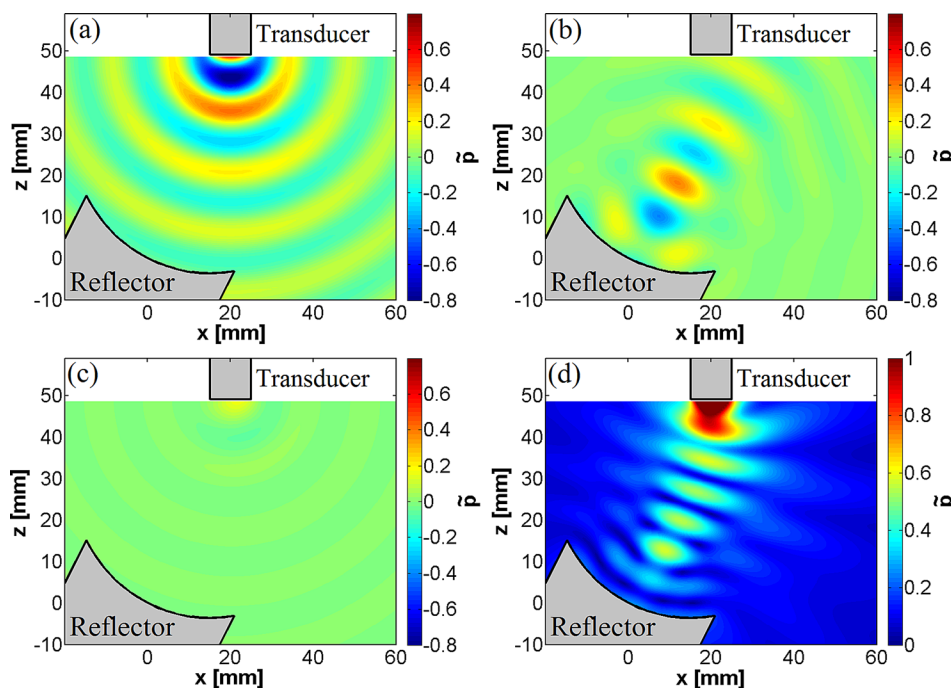

FIG. 2. Sound pressure distribution in the acoustic levitator: (a) Wave emitted by the transducer; (b) wave after the first reflection at the reflector surface; (c) wave after the second reflection; and (d) modulus of the sum of the three previous waves.

transducer radius is that the emitted wave is almost spherical, which means that the reflector can be tilted and displaced off-axis, as shown in Fig. 2.

There are different forms of reducing the amplitudes of the high-order reflections in order to obtain a non-resonant device, such as minimizing the transducer reflection coefficient,[20] reducing the reflector size,[16,17] or by producing two sound beams that are not reflected by the opposite transducers.[19] In the present device, high-order reflections are minimized through the reduction of the transducer radius and by limiting the minimum separation distance between the transducer and the reflector to $d = 50$ mm. Although in most levitators a concave reflector is used to increase the amplitudes of the high-order reflections, it was verified numerically that due to the small transducer radius, the amplitudes of the high-order reflections are not significantly affected by the concave reflector.

After obtaining the sound pressure distribution by the matrix method, Eq. (2) was applied in order to find the Gor'kov potential $\tilde{U}$ for different values of d, L, and θ. The Gor'kov potentials for three different levitator configurations are presented in Fig. 3. This figure also presents a picture of four levitating particles for each simulated configuration. The comparison between the numerical and experimental results of Fig. 3 shows that the positions of minimum Gor'kov potential agree with the experimental levitation

positions. The flattened potential wells of Fig. 3 show that the axial acoustic forces that act on the particles are higher than the lateral forces. Due to the concavity of the reflector surface, the two lower potential wells ($z \approx 20.0$ mm and $z \approx 27.5$ mm) present a higher lateral force than the two upper ones ($z \approx 35.2$ mm and $z \approx 42.8$ mm). In all the pictures, the bottom levitated particle lies at a distance of approximately 20 mm of the reflector surface. The particle in this position can be transported by maintaining the transducer at a fixed position and moving the reflector position up and down. It was also verified that parameters d, L, and θ can be changed during levitation operation, in contrast to other single-axis levitators, where the levitation is lost when the separation distance is switched from one resonance distance to another. It is interesting to note that the particles are arranged in a circular fashion in Fig. 3(c). This distribution of levitating particles is similar to that observed by Kozuka et al.,[19] and it is caused by the destructive interference between the near spherical emitted wave and the wave reflected by the concave reflector.

The matrix method was also applied to investigate the influence of the separation distance between the transducer and the reflector on the acoustic radiation force that acts on the levitated particle. In this analysis, parameters L and θ were set to zero. The dimensionless Gor'kov potential along the z-axis for $d = 50$ mm, 75 mm, and 100 mm is presented in Fig. 4. The three curves present different potential wells with a minimum at $z \approx 20.0$ mm, $z \approx 27.5$ mm, $z \approx 35.2$ mm, and $z \approx 42.8$ mm. These positions of minimum Gor'kov potential do not change significantly when changing the distance d from 50 mm to 100 mm. Moreover, the acoustic radiation force that acts on each particle is sufficient to counteract the gravity in all the distance range between 50 mm and 100 mm. Therefore, levitating particles can be transported by keeping the transducer in a fixed position and translating the reflector vertically from 50 mm to 100 mm. Although there are two points of minimum acoustic potential below $z = 20$ mm, the lateral acoustic radiation force is weak for
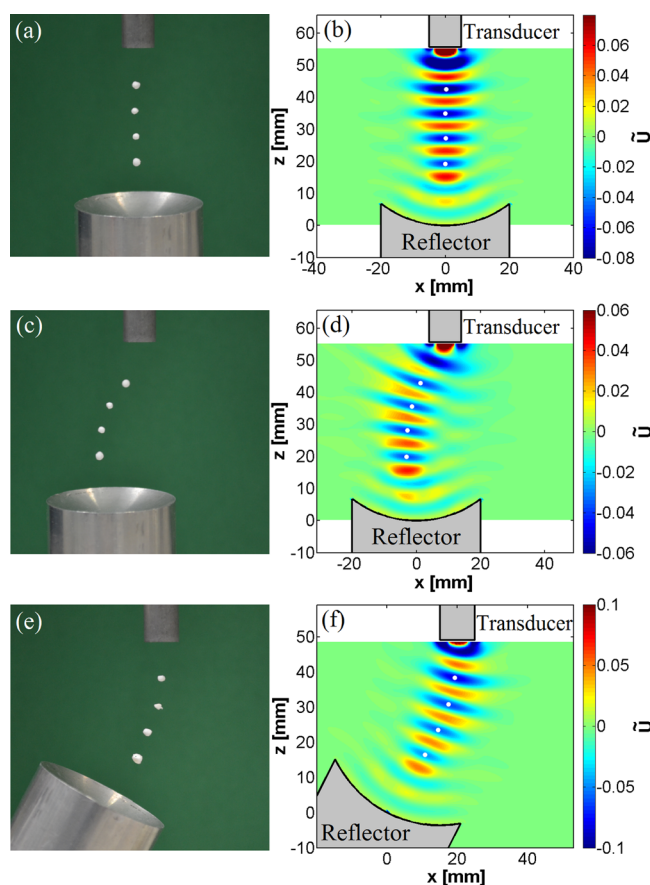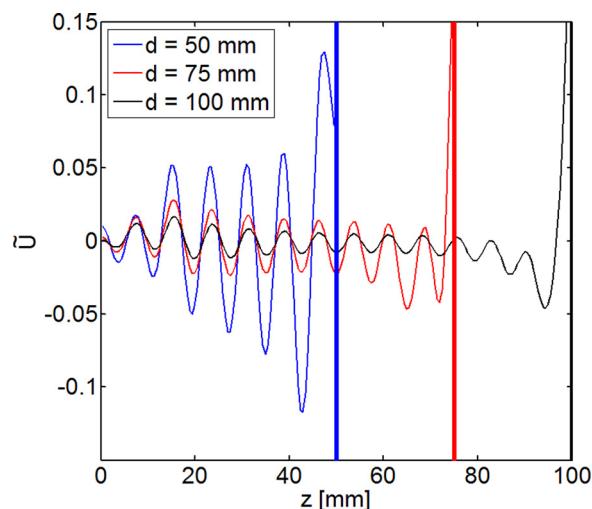

FIG. 3. Acoustic levitation of expanded polystyrene particles and the dimensionless Gor'kov potential for three levitator configurations: [(a) and (b)] $d = 55.7$ mm, $L = 0$, and $\theta = 0°$; [(b) and (c)] $d = 55.7$ mm, $L = 9$ mm, and $\theta = 0°$; and [(e) and (f)] $d = 49.0$ mm, $L = 20$ mm, and $\theta = 27°$.

FIG. 4. Simulated Gor'kov potential along the z-axis for three different separation distances between the transducer and the reflector. The simulations were performed by considering $L = 0$ and $\theta = 0°$.

these two points, and small perturbations can lead the levitating particle to fall on the reflector.

Figure 4 also shows that for a distance $d = 50$ mm, the potential wells of $z \approx 35.2$ mm and $z \approx 42.8$ mm are deeper than the potential wells located at $z \approx 20.0$ mm and $z \approx 27.5$ mm. However, when the distance d is increased to values above 75 mm, the potential wells located at $z \approx 20.0$ mm and $z \approx 27.5$ mm become deeper, which means that these two potential wells provide higher axial forces in the distance range between 50 mm and 100 mm. The other advantage of these two wells is that they present greater lateral forces than the $z \approx 35.2$ mm and $z \approx 42.8$ mm wells, which is important when tilting the reflector. Therefore, the two potential wells located at $z \approx 20.0$ mm and $z \approx 27.5$ mm present greater levitation stability and they are the best for manipulation purposes, as demonstrated in the video (Fig. 1).

In summary, we presented a single-axis acoustic levitator where the separation distance between the transducer and the reflector can be adjusted continually, without requiring the distance to be carefully adjusted to match a resonance condition. The levitator behavior was analyzed by using a numerical model that combines a matrix method based on the Rayleigh integral with the Gor'kov theory. With the numerical simulation, we observed that the standing wave is basically formed by the superposition of two traveling waves: the emitted wave by the transducer surface and the reflected wave by the reflector surface. The numerical simulation showed that the potential wells located at $z \approx 20.0$ mm and $z \approx 27.5$ mm present greater axial and lateral stability than the other wells in the distance range between 50 mm and 100 mm. The proposed levitator geometry can be a simple alternative for the noncontact manipulation of small particles.

[1]E. H. Brandt, Nature **413**, 474–475 (2001).
[2]A. Scheeline and R. L. Behrens, Biophys. Chem. **165**, 1 (2012).
[3]S. Santesson, J. Johansson, L. S. Taylor, L. Levander, S. Fox, M. Sepaniak, and S. Nilsson, Anal. Chem. **75**, 2177 (2003).
[4]S. Santesson and S. Nilsson, "Airborne chemistry: Acoustic levitation in chemical analysis," Anal. Bioanal. Chem. **378**, 1704 (2004).
[5]R. J. K. Weber, C. J. Benmore, S. K. Tumber, A. N. Tailor, C. A. Rey, L. S. Taylor, and S. R. Byrn, Eur. Biophys. J. **41**, 397 (2012).
[6]C. J. Benmore and J. K. R. Weber, Phys. Rev. X **1**, 011004 (2011).
[7]V. Vandaele, A. Delchambre, and P. Lambert, J. Appl. Phys. **109**, 124901 (2011).
[8]J. R. Gao, C. D. Cao, and B. Wei, Adv. Space Res. **24**, 1293 (1999).
[9]W. J. Xie, C. D. Cao, Y. J. Lü, Z. Y. Hong, and B. Wei, Appl. Phys. Lett. **89**, 214102 (2006).
[10]D. Koyama and K. Nakamura, IEEE Trans. Ultrason. Ferroelectr. Freq. Control **57**, 1152 (2010).
[11]D. Foresti, M. Nabavi, M. Klingauf, A. Ferrari, and D. Poulikakos, Proc. Natl. Acad. Sci. U. S. A. **110**, 12549 (2013).
[12]D. Foresti and D. Poulikakos, Phys. Rev. Lett. **112**, 024301 (2014).
[13]T. Hoshi, Y. Oachi, and J. Rekimoto, Jpn. J. Appl. Phys., Part 1 **53**, 07KE07 (2014).
[14]S. A. Seah, B. W. Drinkwater, T. Carter, R. Malkin, and S. Subramanian, IEEE Trans. Ultrason. Ferroelectr. Freq. Control **61**, 1233 (2014).
[15]W. J. Xie and B. Wei, Appl. Phys. Lett. **79**, 881 (2001).
[16]C. A. Rey, U.S. patent 4,284,403 (18 August 1981).
[17]C. A. Rey, D. R. Merkley, G. R. Hammarlund, and T. J. Danley, Metall. Mater. Trans. A **19**, 2619 (1988).
[18]A. Haake and J. Dual, Ultrasonics **40**, 317 (2002).
[19]T. Kozuka, K. Yasui, T. Tuziuti, A. Towata, and Y. Iida, Jpn. J. Appl. Phys., Part 1 **46**, 4948 (2007).
[20]A. Grinenko, C. K. Ong, C. R. P. Courtney, P. D. Wilcox, and B. W. Drinkwater, Appl. Phys. Lett. **101**, 233501 (2012).
[21]L. P. Gor'kov, Sov. Phys.-Dokl. **6**, 773 (1962).
[22]M. A. B. Andrade, N. Pérez, F. Buiochi, and J. C. Adamowski, IEEE Trans. Ultrason. Ferroelectr. Freq. Control **58**, 1674 (2011).
[23]A. Stindt, M. A. B. Andrade, M. Albrecht, J. C. Adamowski, U. Panne, and J. Riedel, Rev. Sci. Instrum. **85**, 015110 (2014).